Supplementary Information for

Improving performance of monolayer arsenene tunnel field-effect transistors by defects

Shun Song,[a,b] Jian Gong,[*a] Hongyu Wen,[b,c] and Shenyuan Yang[*b,c]

[a]*School of Physics and Technology, Inner Mongolia University, Hohhot 010021, P. R. China*

[b]*State Key Laboratory of Superlattices and Microstructures, Institute of Semiconductors, Chinese Academy of Sciences, Beijing 100083, P. R. China*

[c]*Center of Materials Science and Optoelectronics Engineering, University of Chinese Academy of Sciences, Beijing 100049, P. R. China*

1. DVs_T defect in arsenene

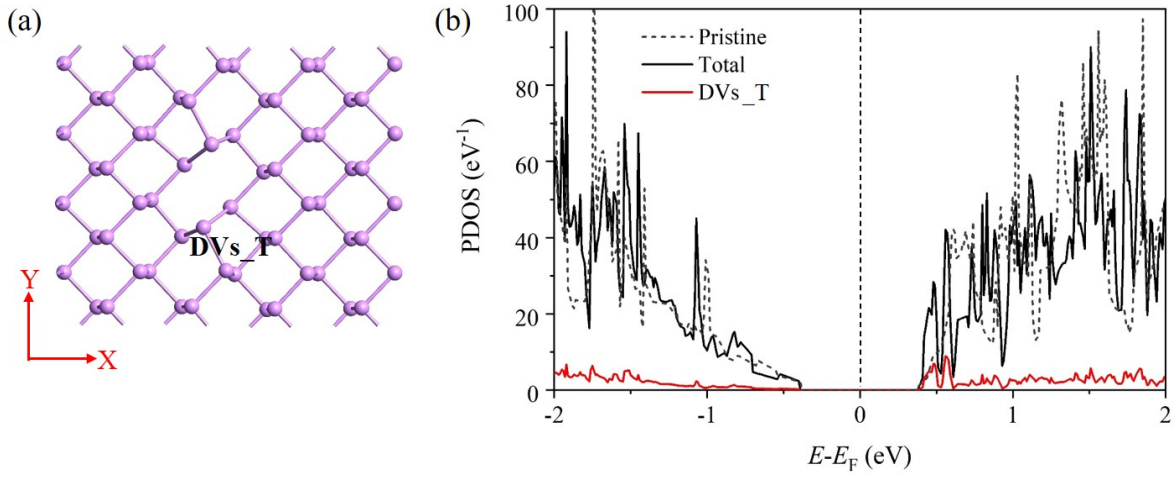

Fig. S1. (a) Double vacancies DVs_T formed by two adjacent top-atoms in arsenene. (b) PDOSs of arsenene monolayer with DVs_T defect.

The DVs_T defect with two adjacent vacancies in the top layer is shown in Fig. S1 (a). Similar to phosphorene [38, 39], the DVs_T is more stable than DVs by 1.1 eV. However, DVs causes small structure distortion around the defect, while DVs_T causes significant structure distortion around it. In arsenene, the adjacent bond length around DVs_T is 2.47-2.63 Å, compared to 2.49-2.51 Å in pristine arsenene. Besides, PDOS

in Fig. S1 (b) shows that the DVs_T defect does not introduce defect states in the band gap region. We speculate that this defect has little contribution to the improvement of the arsenene devices and would not introduce this defect to the arsenene TFET devices.

2. 2H defects in arsenene monolayer

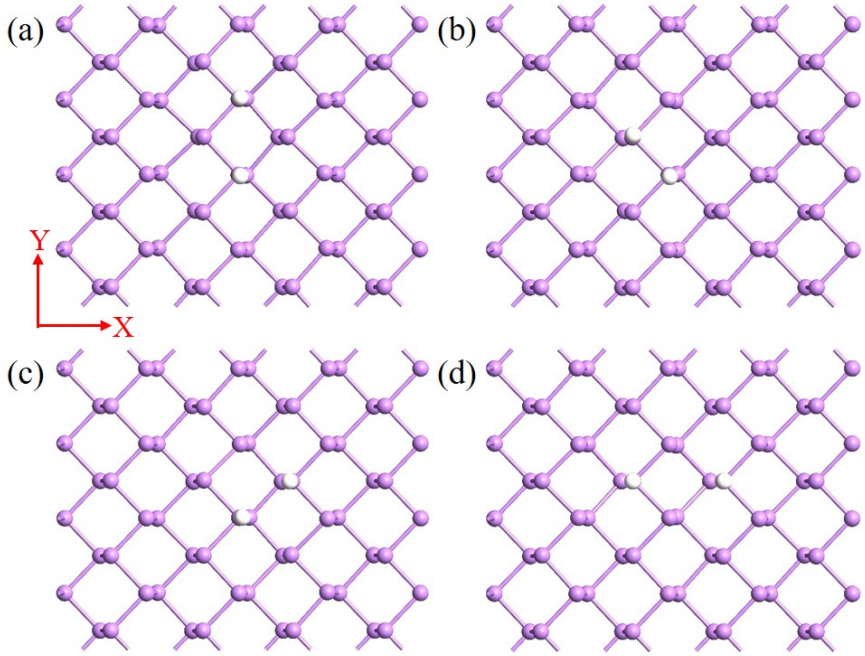

Fig. S2. Four different 2H defects in arsenene monolayer.

We obtain four stable configurations for two H adatoms as shown in Fig. S3 (a)-(d), denoted as 2H_a, 2H_b, 2H_c, and 2H_d. In 2H_b structure, the two H atoms are adsorbed on two bonded As atoms. In 2H_b structure, the two H atoms are adsorbed on two unbonded As atoms in the top layer. The adsorption energies of the four 2H defects are quite similar to each other (-3.25~-3.53 eV), indicating that they have similar stableness. The PDOSs of the four 2H defects are shown in Fig. S3 (a)-(d). The PDOS of 2H_a has been shown in Fig. 2 (d) in the original manuscript. Here we also show it in Fig. S3 (a) for better comparison. It can be seen that the four 2H defects have different electronic structures. Similar to the 2H_a defect, both 2H_b and 2H_d defects introduce mid-gap states in the band gap region, while 2H_c defect introduces a defect state just below the CBM. Therefore, 2H_c defect may not be beneficial to the device transport performance.

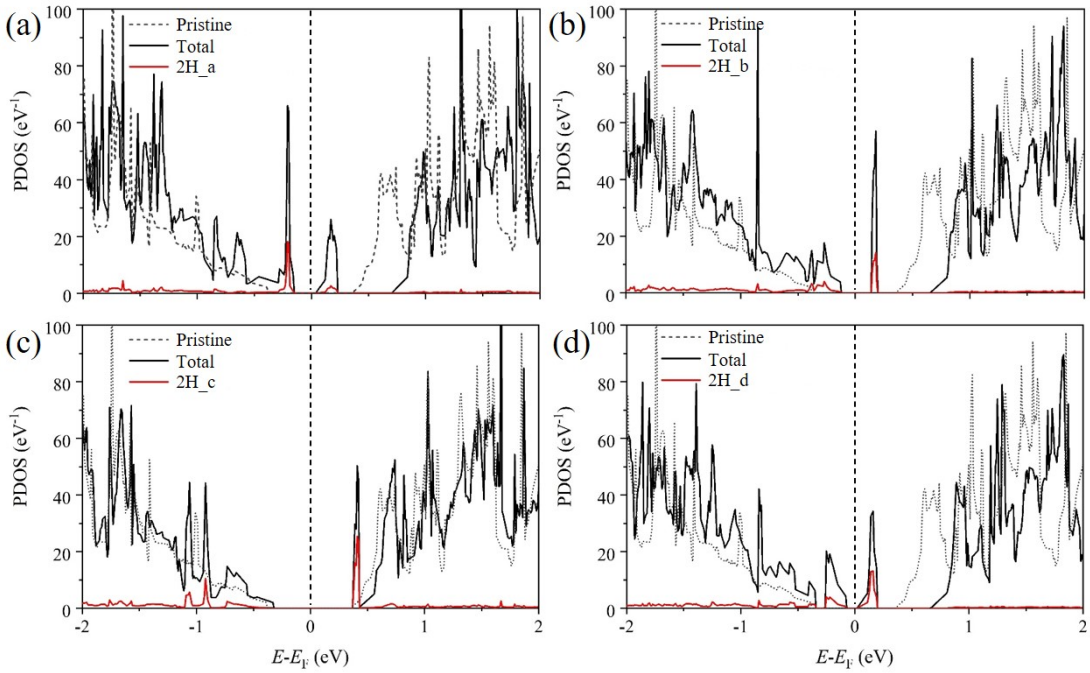

Fig. S3. PDOSs of four different 2H defects in arsenene monolayer.

3. Current-voltage characteristics of TFET devices with 2H defects

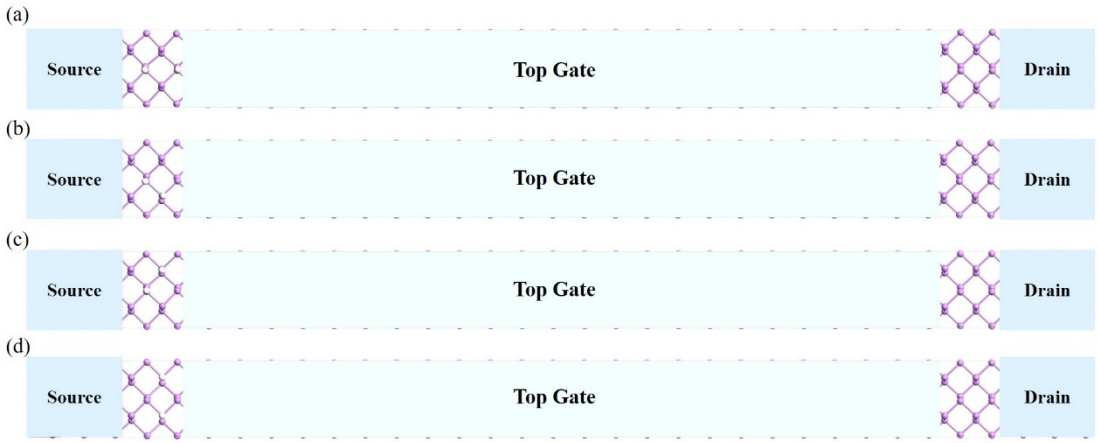

Fig. S4. Schematics of the double gate arsenene TFET devices along the zigzag directions with different 2H defects at the source-channel interface.

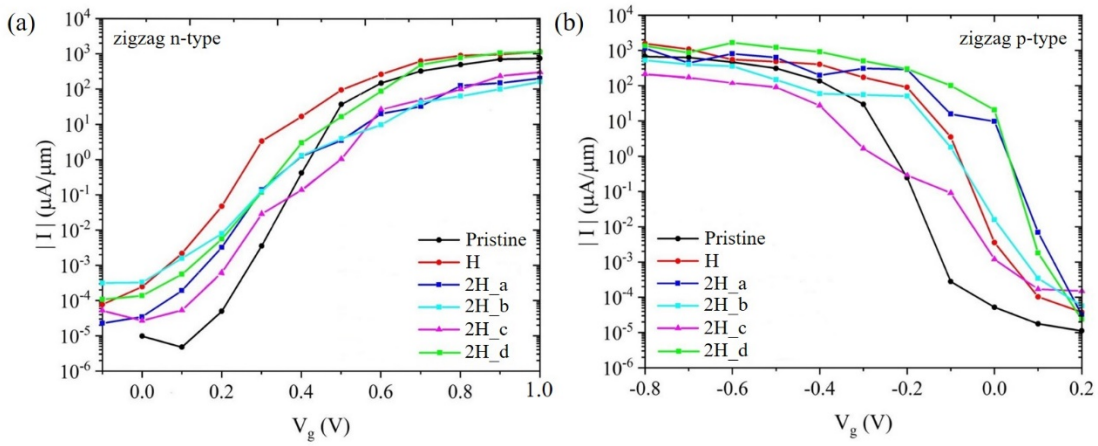

Fig. S5. Current-voltage characteristics of the arsenene TFET devices along the zigzag direction with different 2H defects.

We then simulate the performance of the TFET devices along zigzag transport direction with different 2H defects at the source-channel interface, as shown in Fig. S4. Their current-voltage characteristics are plotted in Fig. S5 and compared to the pristine devices and the devices with one H adatom. As summarized in Table S1, 2H defects could partially improve the performance of the devices. For example, the n-type and p-type devices with 2H_a defect, and the p-type devices with 2H_b and 2H_c defect all have SS values below 60 mV/decade. The SS value of the p-type devices with 2H_d defect can even reach 25 mV/decade. However, the ON-state currents of all the devices are smaller than those with one H defect. The ON-state currents of both n-type and p-type devices with 2H_d defect are the largest due to the defect states near the Fermi level. But the ON-state currents are still below the ITRS 2022 requirement of 1330 $\mu A/\mu m$ for HP devices. We can conclude that the 2H defects cannot further improve the device performance.

Table S1 Summary of the performance of arsenene TFET devices along zigzag direction with single H defect and different 2H defects. The ITRS 2022 targets for HP and LP devices at the 8.8 nm technology node are presented for comparison.

defects	devices	SS (mV/decade)	I_{OFF} (μA/μm)	I_{ON} (μA/μm)	I_{ON}/I_{OFF}
pristine	n-type	49	2×10^{-5}	707	3.54×10^{7}
	p-type	34	2×10^{-5}	500	2.50×10^{7}
H	n-type	56	0.1	1160	1.16×10^{4}
	p-type	34	0.1	1563	1.56×10^{4}
2H_a	n-type	57	0.1	201	2.01×10^{3}
	p-type	31	0.1	942	9.42×10^{3}
2H_b	n-type	80	0.1	521	5.21×10^{3}
	p-type	50	0.1	160	1.60×10^{3}
2H_c	n-type	63	0.1	411	4.11×10^{3}
	p-type	56	0.1	212	2.12×10^{3}
2H_d	n-type	69	0.1	1120	1.12×10^{4}
	p-type	25	0.1	864	8.64×10^{3}
ITRS 2022 HP			0.1	1330	1.33×10^{4}
ITRS 2022 LP			2×10^{-5}	461	2.31×10^{7}